

A Compact High Voltage Nanosecond Pulse Generator

Drew Campbell, Jason Harper, Vinodhkumar Natham, Funian Xiao, and Raji Sundararajan

Electrical & Computer Engineering Technology Dept.
Purdue University, W. Lafayette, IN 47907
email: raji@purdue.edu

Abstract- Application of Pulsed Electric Field (PEF) has been gaining momentum to preserve the quality of foods, such as to improve the shelf-life of bread, milk, orange juice, liquid eggs, and apple juice, and the fermentation properties of brewer's yeast. A pulse generator (pulser) is an integral part of this system. This paper presents the design, building and testing of a compact, portable high voltage MOSFET-based nanosecond pulser in our lab. This high voltage nanosecond pulser has variable pulse widths ranging from 20ns to 20 μ s with a variable pulse potential magnitude of up to 1kV. The high voltage nanosecond pulser is powered from a 9.6VDC rechargeable battery and measures just 4" x 4" x 2". Various fruit juices, including fresh orange and lime juices were studied using this pulser. Results indicate that 1kV/cm, nanosecond pulses could be used for enhancing the longevity of fruit juices at ambient temperatures.

I. INTRODUCTION

The concept of applying external methods to preserve food for longer durations of time has been a constant challenge since the cave days. Over the years many methods were tried, tested and used to achieve this goal. Some of these methods include drying, smoking, cooling, freezing, fermenting, salting, pickling, and canning. With the use of modern technologies and arduous research, newer ways of food preservation are emerging which enable us to further increase the longevity of food products. One such method is applying electrical voltage pulses to control the level of harmful bacterial content in juices [1-5].

Modern methods for preparing juices try to create as many hurdles to bacterial growth and survival as possible. Figure 1 illustrates this [6]. In most of the cases the bacterial growth increases rapidly as soon as the containers containing these juices are opened. The time taken from the instant the juice is opened to the time for it to be completely consumed is when the juice is most favorable to bacterial growth.

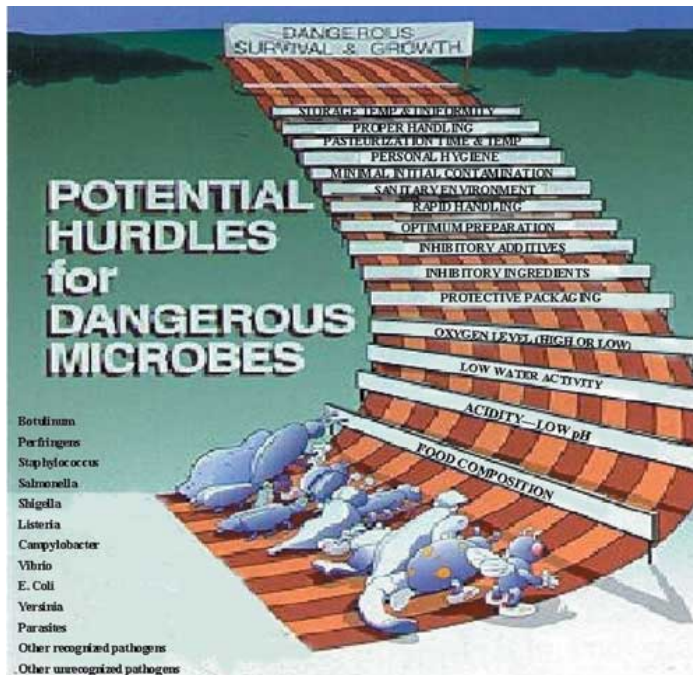


Fig. 1. The various hurdles to bacterial grown and survival [6]

In case of unpasteurized juices, the risk of harmful bacterial presence and growth is even greater. In this research, it is proposed to extend the life expectancy of liquid food, such as fresh juices and commercial/processed juices available in the market using electrical pulses [2, 7-10].

High intensity, short duration pulsed electric field application for processing liquid food, such as juices, has the advantage that the heating effect is significantly less compared to conventional “thermal” processes and more desirable than chemical processes [2,7-10]. A range of electric field values have been used by previous researches, such as from a few kV/cm to tens of kV/cm. The US Food and Drug Administration’s note [1] indicates the use of 15kV/cm and 32kV/cm intensity electric field for orange juice. It is mentioned that an electric field of 50kV/cm was used for apple juice. The shelf life of raw skim milk was studied by Fernandez-Molina et al, using 30 pulses at 40kV/cm, and treatment time of 2 μ s using exponential pulses [5]. While this method has been found to increase the shelf life of these foods, it also introduces some drawbacks. In order to produce high magnitude electric fields, large, costly power supplies are required. Also, high magnitude electric fields cause a significant increase in temperature, having an adverse affect on the flavor of the food. Hence, alternative

techniques are needed and this research addresses that issue using a using low intensity (1000V/cm), nanosecond pulses.

A pulser is an integral part of the electrical pasteurization system and to meet the new requirements of low intensity, nanosecond pulses, a 0 to 1000V, compact, fast RF MOSFET-based nanopulser was designed and developed. This paper presents the details of the innovative design used in building the pulser.

II. DESIGN AND BUILDING OF THE PULSER

The objective of this research was to develop a 0 to 1000V, compact, MOSFET-based nanosecond pulser (Nanopulser) that could operate using a 9.6VDC Rechargeable Battery, with variable pulse durations of 20ns to 20 μ s and with variable pulse repetition rate (PRF) of 1 kHz to 6 kHz. The compact nanopulser can be broken down into three system blocks: 1) high voltage source block which converts the battery's 9.6VDC to a variable high voltage output and stores this charge for use when the pulsing begins, b) the switching block, which is a MOSFET based low-side switch that applies short nanosecond pulses to the load, and 3) the pulse generation block that generates a short nanosecond pulse and supplies enough current to adequately turn the MOSFET on fast enough to apply a nanosecond pulse to the load.

A. High Voltage Source Block

One goal of this project was to keep the pulser as small as possible and make it portable. To achieve this, high voltage DC-DC converters were used. These high voltage modules convert 0-12V_{DC} to 0-1500V_{DC}. The battery voltage is supplied to an adjustable voltage regulator and then to the high voltage module. A potentiometer is used in the design to adjust the regulator voltage to approximately 8V_{DC} to achieve an output voltage of roughly 1000V. Two diodes were used on the output of the high voltage module to protect it from transient spikes and damage. The high voltage module is rated at 10W; therefore a 150k Ω resistor is used to limit the current of the module to 6.6mA to not exceed the rated output power limitation of the module. The module charges a 1 μ F capacitor, which is used to provide energy to the load when pulsed.

B. Nanosecond switch Block

The design specifications require pulse durations as low as 20 nanoseconds (ns); therefore an extremely fast RF MOSFET (IXZR08N120B RF Power MOSFET) by IXYS was chosen as the switch. It is rated at 1200V. A high current driver was used to switch the MOSFET. A driver is needed because of the initial high current drawn to charge the MOSFET gate capacitance of 1960pF. The driver also has to be very fast, so a 4ns rise time MOSFET driver (DEIS420) was chosen. Fig. 2 shows these parts.

The MOSFET driver is powered using the battery with no regulation. Three different capacitance range bypass capacitors are used to filter the power supply to the MOSFET driver. Different capacitance ranges are used to cover different impedance ranges to help

filter out high frequency noise. The CMOS/TTL input of the MOSFET driver is connected to the pulse generation circuit output. The MOSFET's source is connected to ground and the drain is connected to the negative side of the load. A fast switching diode is placed across the load to reduce ringing on the load. The schematic of the nanosecond switch block schematic can be seen in Figure 3.

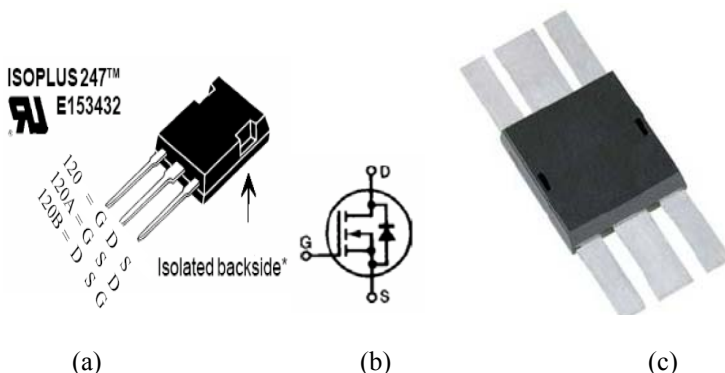


Fig. 2. a) IXZR08N120B-N channel Enhancement mode switch mode RF MOSFET, rated at 1200V and 8A and RDS (on) is 2.1 Ω , (b) MOSFET symbol, and (c) MOSFET Driver DEIC420

C. Pulse Generation Block

A nanosecond pulse generator circuit was constructed using two CMOS digital ICs based on a published report [11]. One IC was a retriggerable monostable multivibrator and the other was a D flip flop. The retriggerable monostable multivibrator produces pulses depending upon the value of one external capacitor and resistor. Since the multivibrator is a dual IC, one can generate two pulses very easily. The pulses can be shifted apart from each other by increasing the external resistance of one multivibrator. A potentiometer is added in series with the external resistor allowing for adjustment to the pulse duration. These pulses are then used to clock and preset the D flip flop. Setting the pulses apart by 20 nanoseconds allows the D flip flop to be clocked high then preset low 20 nanoseconds later. The retriggerable monostable multivibrator needs a clock signal to repeat pulses. A simple 555 timer was used to create a CMOS clock of 1.5 kHz. The 555 timer was also built with potentiometers to allow adjustment of the frequency and duty cycle. All three ICs were powered using a simple 5V_{DC} regulator.

III. PCB LAYOUT DESCRIPTION

The top copper of the PCB contains the majority of the components and trace routes. Most of the nanosecond switching and pulse generation blocks are laid out on the top layer. Placement of components was closely watched to reduce critical route lengths and

crosstalk. The pulse generation block is positioned on the bottom left of the board. Three traces in the pulse generation block were closely watched during the routing phase. The first important trace is the clock signal coming from the 555 timer. This trace was routed as directly as possible to allow good signal path to the retriggerable monostable multivibrator. The other two traces are the pulses from the retriggerable monostable multivibrator clocking and presetting the D flip flop. The length and width of these traces were monitored to prevent signal loss or degradation. The external resistor and capacitor were positioned close to the retriggerable monostable multivibrator to create accurate calculated pulses.

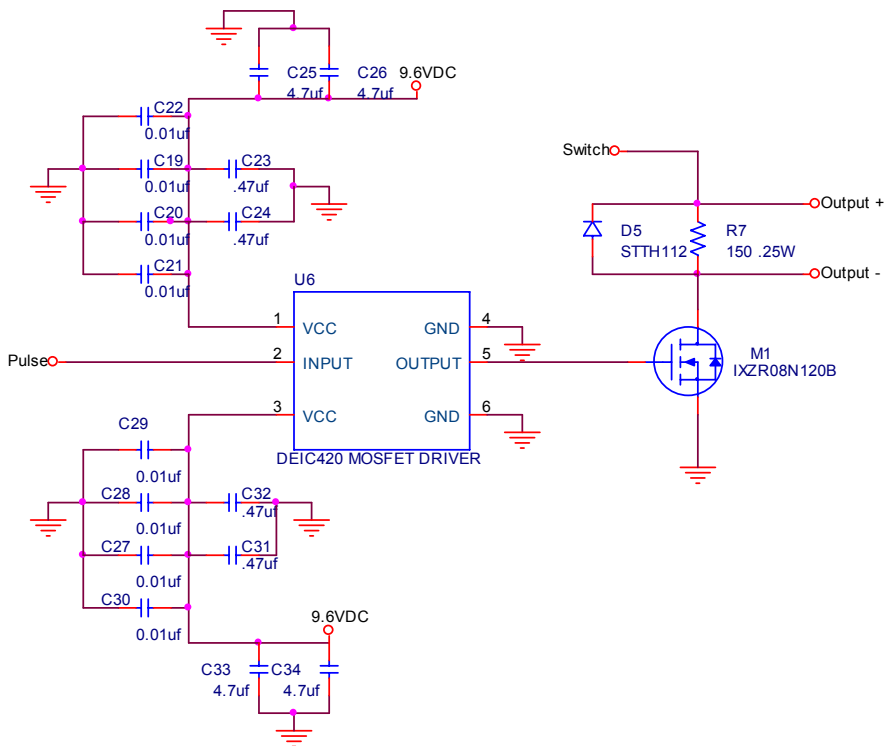


Fig. 3. Nanosecond Switch Block Schematic

The nanosecond switching block is located in the bottom middle and right side of the PCB. Many of these traces were made very wide for good signal quality. Also since such high voltages were used the distance between traces was closely watched. It was determined that around 100 mils of clearance was needed to prevent arcing between high voltage traces and ground. Ground signals were also made wide to help reduce ground

paths. Two traces were closely watched in this section. First the 20 nanosecond pulse from the pulse generation block was routed directly to the MOSFET driver with very short wide traces.

Input power from the battery enters the board on a connector on the top left of the PCB. Two switch connectors are also positioned in the same area. One switch is used for on/off power and the other turns the pulse generation block on/off. Also the board is cut out near the jacks to allow them to sit level with the board to be soldered. Many vias were added to the ground traces of the circuit. These vias allowed good paths to the ground plane on the bottom layer. Fig. 4 shows the top PCB layout.

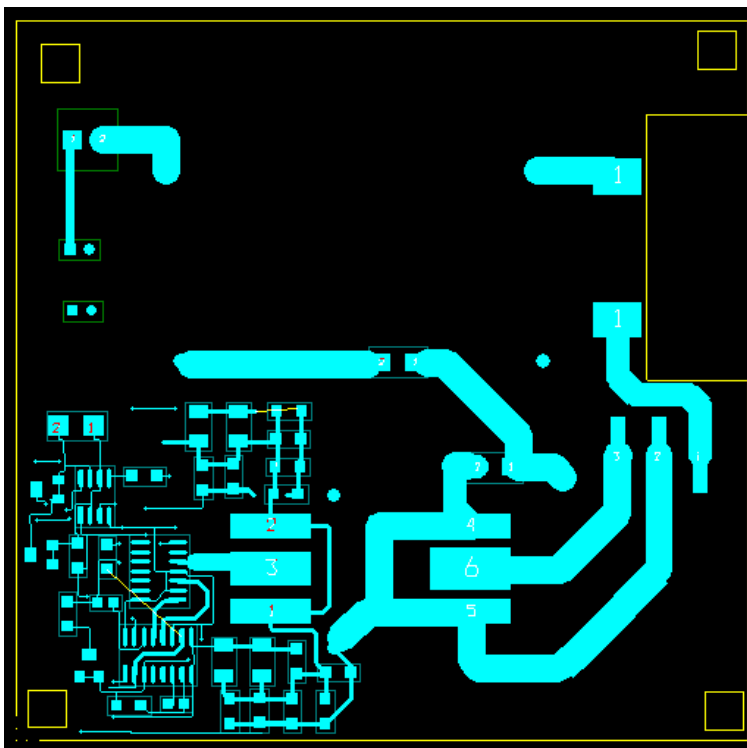


Fig. 4. Top Copper Layout

The bottom copper of the PCB was used for the power supplies, high voltage source block, and ground plane. Placement was again important in many of the components. The power supplies for the pulser are positioned on the left side of the PCB. One power supply is set at $5V_{DC}$ for powering ICs and the other is adjustable for the power input of the high voltage module. Fig. 5 shows a photograph of the pulser. The 1000V capacitor

is on the right and the MOSFET is on the left. Fig. 6 shows a layout diagram of the pulser.



Fig. 5 4"x4"x2" Compact MOSFET Nanopulser

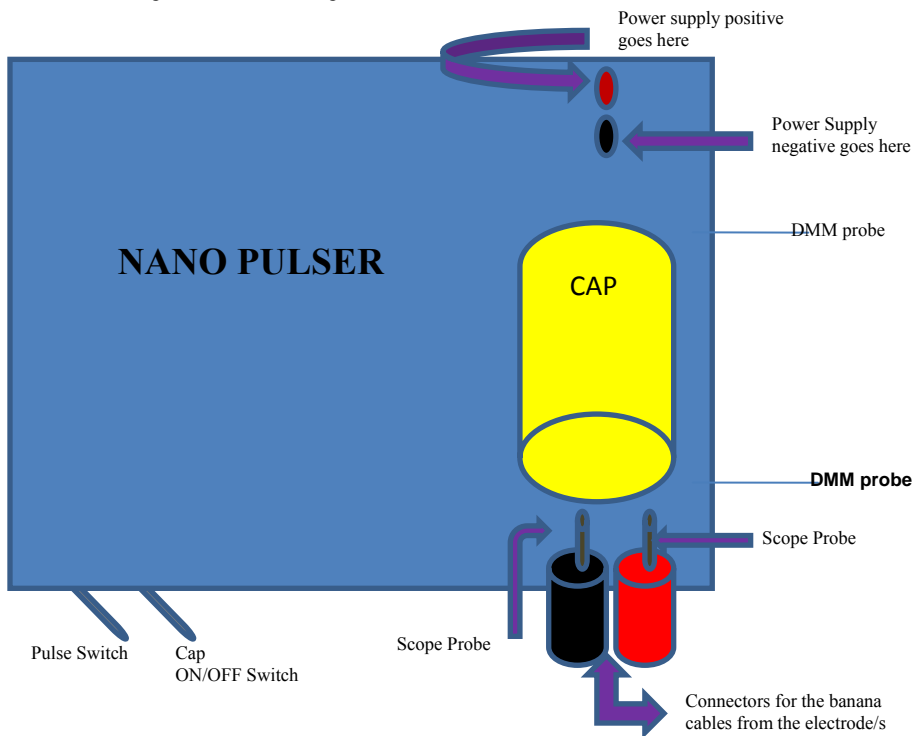


Fig. 6. Illustration of the Nanopulser Connections

IV. RESULTS & DISCUSSION

A. Output Voltage Waveform Measurements

Fig. 7 shows the 555 timer clock signal for the retriggerable monostable multivibrator. This clock signal is CMOS and TTL compatible. The spikes seen on the rising edge of the signal were eliminated in later tuning. These spikes did not seem to affect the circuit operation nor is its cause known. The load pulse was very successful and created a clean 20 nanosecond pulse. Very little ringing was seen and the signal should work well for most pulser applications. Figs. 8 (a) and (b) show output voltage waveform for fresh lime and fresh mango juices respectively.

Fig. 9 shows compares the rise time (4.8ns) of the output voltage waveform obtained in this project with the rise time (3ns) of the driver as shown in the manufacturer's data sheet. Since the manufacturer's testing conditions are unknown, this correlation is considered very good.

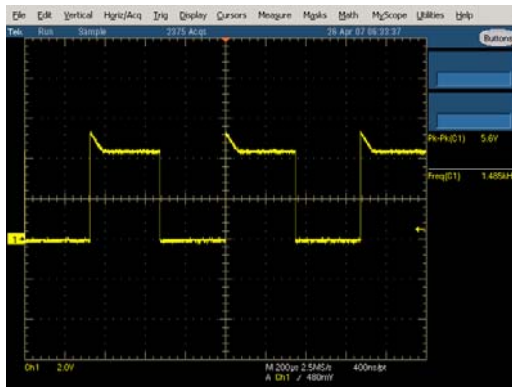
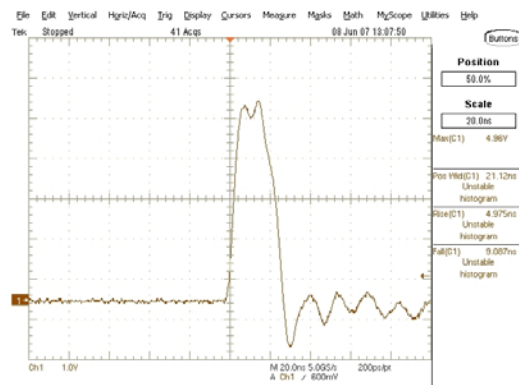
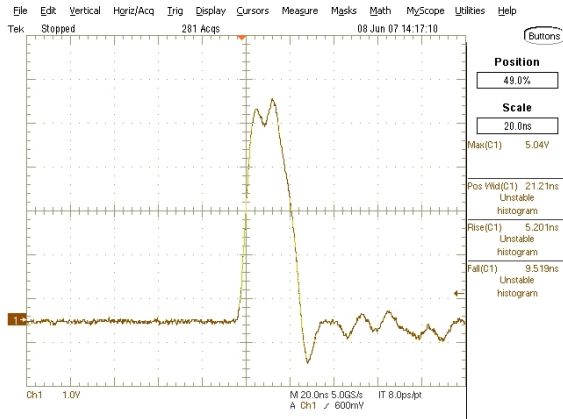


Fig. 7. 555 Timer Output Signal

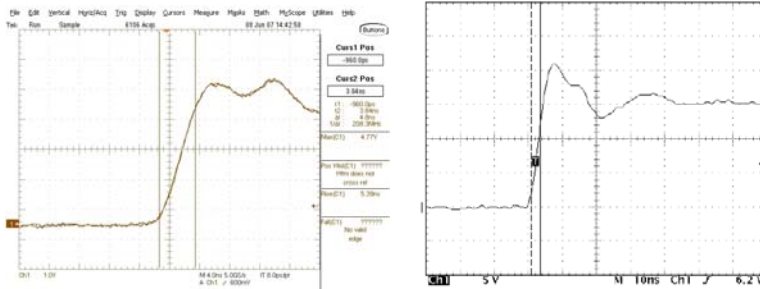


(a) Fresh Lime juice - 496V across 0.4cm cuvette (1240V/cm).



(b) Fresh Mango juice - 500V across 0.4cm cuvette (1250V/cm).

Fig. 8 Output voltage pulse waveforms for freshly squeezed Lime and Mango juices. The horizontal scale is 20ns per division. The vertical scale is 1V per division. The pulse width is about 20ns. The waveform was recorded using a Tektronix TDS 5032B , 300MHz, 5MS/s Digital Storage Scope and a 100x probe.



(a) 4.8ns output waveform

(b) 3ns Driver Output Waveform by Manufacturer

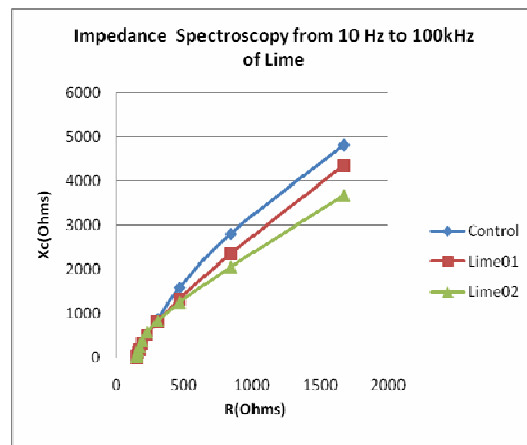
Fig. 9 MOSFET Driver output waveform obtained in this project vs that of the manufacturer

B. Impedance Spectroscopy Measurements

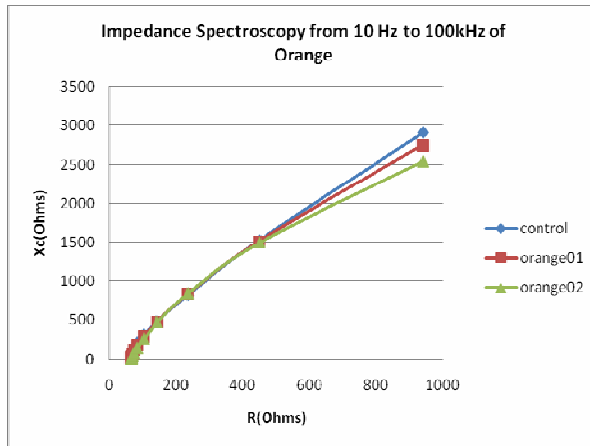
Impedance Spectroscopy (IS) is a widely used technique for measuring electrochemical phenomena on solid, porous, synthetic and biological materials, such as breast tumors, ripening of kiwifruit, and other tissues [12-20]. IS measures the electrical properties of any material, i.e. the conductance (or resistance) and the reactance as a function of applied alternative current (ac) frequency. Cole-Cole plot (resistance vs reactance) is used to arrive at RC equivalent circuits and their values [19]. The main advantage of this technique is that it can provide information on the state of material. IS is an ac measurement technique in which the ratio of voltage and current is measured over a range of frequencies. It is a non-invasive, nondestructive test technique in which very little energy need be dissipated by the system under test, leaving it virtually unaffected. This

method is useful to characterize cellular changes quantitatively. It can be used as a method of identifying and following detectable cellular responses, in ex vivo, in vivo and in vitro [15-20].

In this study, it was used to characterize the impedance change due to applied pulses. Autolab PGSTAT 12 impedance analyzer was used. It gives 40 data points for a frequency range from 0.5Hz to 100kHz. Figs. 10a and b show the variation of pulsed fresh lime and orange juices with respect to the unpulsed juice (control). Conditions 1 and 2 correspond to 10 minutes and 20 minutes of pulse applications respectively. A 0.4cm electrode gap was used for this measurement. The applied voltage was 500V (corresponding to a electric field intensity of 1250V/cm). The trend of variation of the control and the pulsed juices is similar except for some small variation in the magnitude especially at low frequencies. Each point in the graph indicates a frequency. Normally, the impedance magnitudes are lower at high frequencies and larger at low frequencies. Thus, the points on the left correspond to data at high frequencies where there is not much change. A look at the quantitative data (not shown) shows that below 100Hz, the variation between the control and pulsed juices started becoming larger. The reduction in impedance indicates the increase in permeability of the pulsed juices compared to the control and it varies at different frequencies indicating the dielectric dispersion of these samples.



(a) Lime Juice



(b) Orange Juice

Fig. 10 Impedance Spectrographs of fresh Lime and Orange juices. 01 and 02 denote duration of pulse applied- 10 and 20 minutes respectively

V. SUMMARY

A compact High Voltage MOSFET-based nanosecond pulser was designed, tested successfully which met all the design specifications. Off the shelf components were used along with the fast, state-of-the-art IXYS MOSFET and its driver. Final cost of the pulser was roughly about a few hundred dollars, which when compared to the price of commercial pulsers is quite inexpensive. Impedance spectroscopy study of the samples at a frequency range of 10Hz to 100kHz showed reduction in the impedance of the pulsed juices compared to unpulsed juice. This might have been caused by the increase in the permeability of the juice samples. More work is in progress to better understand the mechanism of electroporation of juices.

ACKNOWLEDGMENTS

We are very grateful to Dr. Kevin Otto and Mr. Ryan Muir of Biomedical Engineering, Purdue University for assistance with the Impedance Spectroscopy measurements.

REFERENCES

- [1] Kinetics of microbial inactivation for alternative food processing technologies-Pulsed Electric Fields”, US Food and Drug Administration, <http://www.cfsan.fda.gov/~comm/ift-pef.html>, Apr 2005
- [2] S.H. Jayaram, “Sterilization of Liquid Foods by Pulsed Electric Fields”, IEEE Electrical Insulation Magazine, Vol. 16, No. 6, Nov/Dec 2000
- [3] T. Grahl and H. Markl, “Killing of microorganisms by pulsed electric fields”, Applied Microbiology and Biotechnology, Vol. 45, No. 1-2, March 1996, pp. 148-157

- [4] R.E. Bruhn, et al., "Heat Conduction in Microbes exposed to Pulsed Electric Fields", IEEE Trans. Dielectrics & Electrical Insulation, Vol. 5, No. 6, Dec 1998
- [5] J. J. Fernandez-Molina, et al., "Shelf-life extension of raw skim milk by combining heat and pulsed electric fields, Food Res. Institute, 1999
- [6] R.P. Bates J.R. Morris and P.G. Crandall, "Principles and practices of small - and medium - scale fruit juice processing", Food Science and Human Nutrition Department University of Florida, United States. <http://www.fao.org/DOCREP/005/Y2515E/y2515e00.htm#toc>
- [7] D. Wetz et al., "Short pulse electric field sterilization of liquid media", Proc. Pulsed Power Conference, 2003, Vol. 2, pp. 1124-1127
- [8] A. El-Hag, S. Jayaram, and M. Griffiths, "Inactivation of naturally grown microorganisms in orange juice using pulsed electric fields", IEEE Trans. Plasma Science, Vol. 34, No. 4, Aug 2006, pp. 1412-1415
- [9] Raji Sundararajan, Anthony Gutierrez, and Gene Harding, "Electrical Pulse- Mediated Sterilization of Fruit Juices", Proc. Electrostatics Society of America (ESA) Annual Conf, 2007.
- [10] Victor Godinez and Raji Sundararajan, "Low Voltage Pulse-Mediates Sterilization of Liquid Food", CEIDP, Oct 2007
- [11] <http://www.edn.com/article/CA46850.html>, Apr 2007
- [12] B.H. Brown, et al., "Detection of cervical intraepithelial neoplasia using impedance spectroscopy: a prospective study", *BJOG: an Intl J of Obstetrics and Gynaecology*, Vol. 112, pp. 802-806, June 2005.
- [13] K.S. Osterman, "Non-invasive assessment of radiation injury with electrical impedance spectroscopy", *Physics in Medicine and Biology*, Vol. 49, pp. 665-683, 2004.
- [14] P. Aberg, et al., "Skin cancer identification using multifrequency electrical impedance-a potential screening tool", *IEEE Trans. Biomed Eng*, Vol. 51, pp. 2097-2102, 2004.
- [15] R.Y. Wang, et al., "Study on fish embryo responses to the treatment of cryoprotective chemicals using impedance spectroscopy", *Eur Biophys J*, 2005.
- [16] T. Suselbeck, et al., "Intravascular electric impedance spectroscopy of atherosclerotic lesions using a new impedance catheter system", *Basic Res. Cardiol*, Vol. 100, pp. 446-452, 2005.
- [17] A. Soley, et al., "On-line monitoring of yeast cell growth by impedance spectroscopy", *Jl of Biotechnology*, Vol. 118, pp. 398-405, 2005.
- [18] E. Gersing, "Impedance spectroscopy on living tissue for determination of the state of organs", *Bioelectrochemistry and Bioenergetics*, Vol. 45, pp. 145-149, 1998.
- [19] A.D. Bauchot, F.R. Harker, and W.M. Arnold, "The use of electrical impedance spectroscopy to assess the physiological condition of kiwifruit", *Postharvest Biotechnology and Technology*, Vol. 18, pp. 9-18, 2000.
- [20] D.A. Dean, T. Ramanathan, D. Machado, and R. Sundararajan, "Electrical impedance spectroscopy study of biological tissues", *Jl of Electrostatics* 66 (2008) 165-177